


# Development of a Microscale Thermophoresis-Based Method for Screening and Characterizing Inhibitors of the Methyl-Lysine Reader Protein MRG15

SLAS Discovery  
1–11  
© Society for Laboratory  
Automation and Screening 2020  
DOI: 10.1177/247255220949166  
journals.sagepub.com/home/jbx  


Alessandra Feoli<sup>1</sup>, Vincenzo Pisapia<sup>1,2,3</sup>, Monica Viviano<sup>1</sup>,  
Sabrina Castellano<sup>1</sup>, Tanja Bartoschik<sup>3</sup>, and Gianluca Sbardella<sup>1</sup> 

## Abstract

MRG15 is a transcription factor containing the methyl-lysine reader chromodomain. Despite its involvement in different physiological and pathological states, to date the role of this protein has not been fully elucidated due to the lack of a specific and potent chemical probe.

In this work, we report the development of a microscale thermophoresis (MST)-based assay for the study of MRG15–ligand binding interactions. After the development, the assay was validated using a small focused library and UNC1215 as the reference compound, to yield the identification of 10 MRG15 ligands with affinities ranging from 37.8 nM to 59.1 μM. Hence, our method is robust, convenient, and fast and could be applied to other methylation reader domain-containing proteins for the identification of new chemical probes.

## Keywords

MRG15, MST, biophysics, epigenetics

## Introduction

A variety of fundamental processes in cells are regulated, either directly or indirectly, by posttranslational modifications occurring on histone proteins. The indirect regulation is mediated by specialized “reader” domains that can identify and bind specific covalent modifications such as, for example, lysine methylation.<sup>1,2</sup> A misregulation of such chromatin-reading capability often occurs in various diseases, including cancer, and as a consequence, methylation reader proteins have gained growing interest in recent years as major targets for drug development.<sup>2,3</sup> One of the most interesting methyl-lysine reader proteins is MRG15 (MORF-related gene on chromosome 15), a chromodomain-containing transcription factor that plays a vital role in embryonic development, cell proliferation, and cellular senescence.<sup>4</sup> It is expressed in a wide variety of human tissues, and its homologs have been identified in many other eukaryotes.<sup>5</sup> Human MRG15 consists of a putative chromodomain (*N*-terminal residues 1–85) and a conserved MRG domain (*C*-terminal residues 151–323), which are linked together by a flexible region (residues 86–150). The MRG domain is highly conserved among all MRG proteins and the crystal structure of the MRG domain of human MRG15 was determined in 2006 (**Fig. 1**).<sup>6,7</sup> MRG15 associates with

both histone acetyltransferases (HATs) and deacetylases (HDACs), and it is involved in the regulation of the chromatin structure through association with these histone-modifying enzymes.<sup>8</sup> Additionally, MRG15 specifically recognizes the methylated H3K36 (H3K36me3) and recruits polypyrimidine tract binding (PTB) protein at intronic splicing silencer elements near an exon to suppress exon insertions into mRNA.<sup>9</sup> Hence, considering all these evidences, it is clear that MRG15 has multiple functions, most of them being still unknown. In this regard, the availability

<sup>1</sup>Department of Pharmacy, Epigenetic Med Chem Lab, University of Salerno, Fisciano, SA, Italy

<sup>2</sup>PhD Program in Drug Discovery and Development, University of Salerno, Fisciano, SA, Italy

<sup>3</sup>NanoTemper Technologies GmbH, Munich, Germany

Received April 10, 2020, and in revised form July 21, 2020. Accepted for publication July 21, 2020.

Supplemental material is available online with this article.

## Corresponding Author:

Gianluca Sbardella, Department of Pharmacy, Epigenetic Med Chem Lab, University of Salerno, Via Giovanni Paolo II 132, Fisciano, SA 84084, Italy.

Email: [gsbardella@unisa.it](mailto:gsbardella@unisa.it)

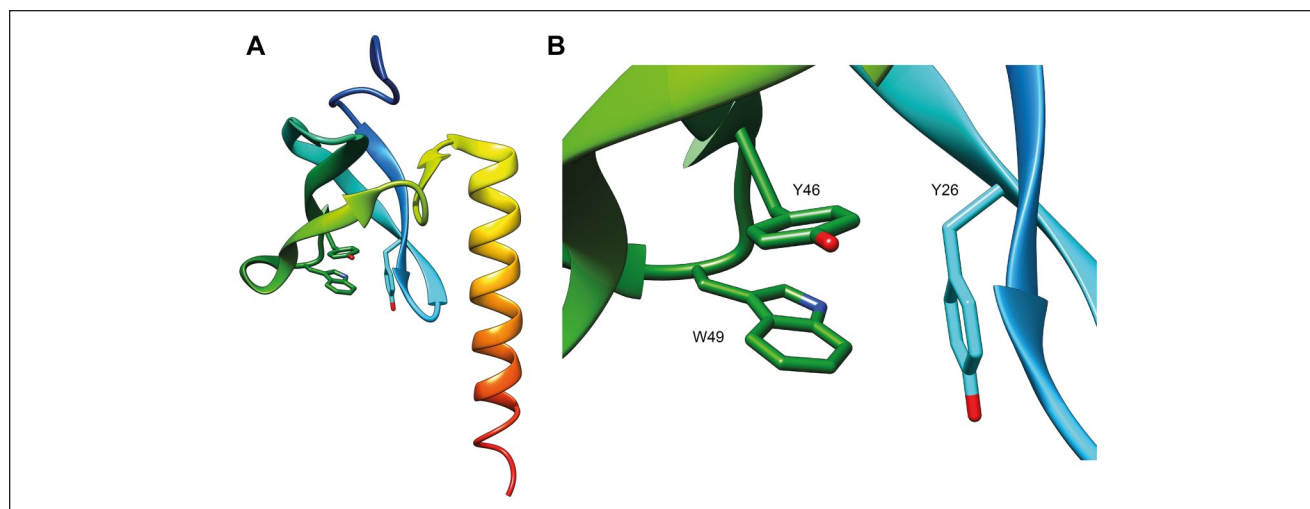


**Figure 1.** (A) Crystal structure of the human MRG15 chromodomain (PDB: 2F5K) with (B) detail of the aromatic cage. The picture was prepared using UCSF Chimera (coordinates from Protein Data Bank, PDB ID code 2F5K).<sup>42</sup>

of chemical probes would help to obtain better insights into its functions in physiological and pathological conditions. Unfortunately, to date no selective chemical probe for this protein has been reported. The only ligand reported thus far is UNC1215, initially identified as a ligand of the MBT domain of the protein L3MBTL3 (isothermal titration calorimetry [ITC]  $K_D = 0.5 \mu\text{M}$ ).<sup>10,11</sup> However, the compound is also able to inhibit (even if with lower affinity) the activity of other reader proteins, such as the Tudor domains of PHF20 (ITC  $K_D = 107 \mu\text{M}$ ), SPIN1 (ITC  $K_D = 101.5 \mu\text{M}$ ), and the chromodomain of MRG15 (ITC  $K_D = 29.1 \mu\text{M}$ ).<sup>10,11</sup>

The relatively low availability of chemical probes is a feature of this class of epigenetic proteins, and it strictly depends on the mechanism of action of readers. Differently from extensively studied writer and eraser enzymes, the inhibition of which represents a rather canonical medicinal chemistry problem, the study of reader proteins is much more complicated because of the weak interaction with native substrates and the superficial binding sites that make the development of selective inhibitors challenging.<sup>2,3,11–14</sup> Moreover, the discovery of new modulators for reader proteins requires the use of techniques suitable for the study of protein–small-molecule interactions. In this regard, many biophysical methods are commonly used in drug discovery programs for the identification of new ligands (each of them with advantages and drawbacks), including differential scanning fluorimetry (DSF), surface plasmon resonance (SPR), ITC, and microscale thermophoresis (MST).

DSF is based on the well-established thermodynamic principle that the thermal stability of a protein, often quantified as the midpoint of thermal denaturation or the melting point ( $T_m$ ), can be altered by a binding ligand.<sup>15,16</sup> DSF is indeed a useful screening method, and provides an easy optimization of assay conditions and fast assay preparation

and data analysis.<sup>15,17</sup> Nevertheless, this method suffers from sensitivity problems, as low-affinity ligands are usually not detected, and furthermore, it is a qualitative method that generally cannot give an indication about the  $K_D$ . Moreover, it is prone to give false negatives, as not all ligands that bind will also lead to a change in the thermal stability, and consequently, a few binders could be missed.

SPR allows the real-time high-sensitivity measurement of interactions by flowing a solution of analyte over the surface of target biomolecules immobilized on a sensor chip.<sup>18–20</sup> Since first introduced in the early 1990s, SPR has been proven to be one of the most powerful technologies to determine specificity, affinity, and kinetic parameters of analyte–ligand interactions. However, the need to immobilize one of the binding partners on the surface of a sensor chip can modify the binding ability of the ligand.<sup>21</sup>

ITC is a robust technique that can measure a wide range of binding affinities.<sup>22</sup> Using this technology, thermodynamic parameters (enthalpy and entropy), as well as binding constants and stoichiometry, can be obtained from a single titration. The major drawback is the requirement of a high quantity of protein for each measurement, meaning that ITC cannot be used for the screening of a large number of compounds.<sup>23</sup>

Among all the reported techniques, MST is the most recently introduced one, even if it is based on the principle of thermophoresis that was already observed and reported by Carl Ludwig in 1856 and further understood by Charles Soret in 1879.<sup>24,25</sup> MST is a biophysical technique that allows us to measure the strength of the interaction between two molecules. It does that by measuring the changes in fluorescence as a result of an infrared laser-induced temperature change. The fluorescence detected can be the intrinsic fluorescence from tryptophan or, most commonly, from a

fluorophore attached to the molecule. There are two components that contribute to the fluorescence change that is measured. One component is thermophoresis, which is the directed movement of molecules within a temperature gradient. Typically, molecules move away from a heat source, but it can also happen in the opposite direction. As molecules move away from the point where the heat is applied, a change in the intensity of the fluorescence is recorded.<sup>26</sup> The other is the major component of the MST signal detected; this is called temperature-related intensity change (TRIC), an effect where the fluorescence intensity of a fluorophore is temperature dependent. This temperature dependency is also related to changes in the local microenvironment of the fluorophore, which can be strongly affected by the binding of a ligand to the fluorescent target molecule.<sup>27</sup>

From different points of view, MST technology is superior to other methods in determining the parameters of molecular interactions; indeed, it requires low sample consumption, it allows a rapid analysis, no surface immobilization is required, and it allows the measurement of interactions in close-to-native protein conditions. In addition, it enables a live detection of sample aggregation, sticking, and precipitation effects.<sup>25</sup>

Herein, we report the development and optimization of a convenient MST assay for the study of MRG15–ligand binding interactions and its feasibility as a robust tool for the identification of new ligands.

## Materials and Methods

### MRG15 Protein Expression and Purification

GST-MRG15 protein (amino acids 1–120) was expressed in BLR(DE3)pLysS cells in lysogeny broth (LB) in the presence of 100 µg/mL ampicillin. Cells were grown at 37 °C to an OD<sub>600</sub> of 0.8, induced by isopropyl-1-thio-*D*-galactopyranoside (IPTG; 100 µM), and incubated overnight at 37 °C. Cells harboring the expressed protein were pelleted at 5000g for 15 min at 4 °C, washed twice with phosphate-buffered saline (PBS), and frozen at –80 °C. For protein purification, the pellet was thawed on ice and suspended in 40 mL of lysis buffer (PBS buffer, pH 7.4) supplemented with a protease inhibitor cocktail. Cells were lysed using a sonicator (Vibra-Cells, Sonics, Newtown, CT; amplitude 30%) for 20 min on ice, and cell debris was pelleted at 10,000g for 30 min at 4 °C. The clarified lysate was filtered using a 0.45 µm syringe filter and loaded onto a 1 mL GSTrap HP column (Cytiva, formerly GE Healthcare Life Sciences, Milan, Italy) at a flow rate of 1 mL/min, previously conditioned with the binding buffer (PBS buffer, pH 7.4). The protein was eluted in isocratic mode using the elution buffer (50 mM Tris-HCl, 10 mM reduced glutathione, pH 8.0). Fractions containing the protein were confirmed by sodium dodecyl sulfate–polyacrylamide gel electrophoresis

(SDS-PAGE), pooled, and dialyzed overnight at 4 °C to remove glutathione.

### Protein Labeling

Fluorescence labeling of MRG15 was performed following the protocol for *N*-hydroxysuccinimide (NHS) coupling of the RED-NHS second-generation dye (MO-L011; NanoTemper Technologies, Munich, Germany) to lysine residues. Briefly, 100 µL of a 20 µM solution of MRG15 protein in labeling buffer (130 mM NaHCO<sub>3</sub>, 50 mM NaCl, pH 8.2) was mixed with 100 µL of 60 µM second-generation dye in labeling buffer and incubated for 30 min at room temperature (r.t.). Unbound fluorophores were removed by size-exclusion chromatography with MST buffer as running buffer. The degree of labeling (DOL) was determined using extinction coefficients  $\epsilon = 65,507 \text{ M}^{-1} \text{ cm}^{-1}$  for the protein and  $\epsilon = 195,000 \text{ M}^{-1} \text{ cm}^{-1}$  for the dye, with a correction factor ( $C_F$ ) of 0.04 at 280 nm and a path length ( $d$ ) of 1 cm, using the following equations:

$$C_{\text{protein}} = [A_{280} - (A_{650} \times C_F)] / \epsilon_{\text{protein}} \times d \quad (1)$$

$$\text{DOL} = A_{650} / \epsilon_{\text{dye}} \times C_{280} \quad (2)$$

where  $C_{\text{protein}}$  = protein concentration,  $A_{280}$  = protein absorbance at 280 nm,  $A_{650}$  = dye absorbance at its maximum  $\lambda$ ,  $\epsilon_{\text{protein}}$  = extinction coefficient of the protein,  $\epsilon_{\text{dye}}$  = extinction coefficient of the dye, and  $d$  = path length of the spectrophotometer.

For storage, MRG15 was frozen in 10 µL aliquots at –80 °C. Prior to MST experiments, aliquots of MRG15 were thawed on ice and centrifuged for 15 min at 4 °C and 12,000g to remove protein aggregates.

### Protein Thermal Stability Measurements

To verify if the labeling of MRG15 with the dye altered the protein integrity, thermal unfolding profiles of both proteins were recorded using Tycho NT.6 (NanoTemper Technologies Munich, Germany). This test was performed using 3 µM protein diluted in MST buffer. Thermal unfolding profiles were recorded from 35 to 95 °C with a thermal ramp of 30 °C/min. The inflection temperature and a profile similarity factor were directly obtained from the Tycho NT.6 instrument.

### Assay Development for MST Screening

The MST experiments were performed on the Monolith NT.115Pico instrument (NanoTemper Technologies) using 5 nM protein concentration, premium coated capillaries, and 20% LED power. Data were analyzed at medium MST

power. Briefly, all small molecules were stored at 50 mM in pure DMSO at  $-20\text{ }^{\circ}\text{C}$ . For small molecules, a 16-step serial dilution was prepared. For this, 10  $\mu\text{L}$  of assay buffer was added to Eppendorf tubes 2–16. Twenty microliters of the highest small-molecule concentration (200  $\mu\text{M}$ , 1% DMSO) was transferred into tube 1. Then 10  $\mu\text{L}$  was transferred from tube 1 to tube 2 and mixed by pipetting up and down. Next, 10  $\mu\text{L}$  was transferred from tube 2 to tube 3 and again mixed by pipetting up and down. This step was repeated for all remaining tubes. Ten microliters was discarded from tube 16. In a next step, 10  $\mu\text{L}$  of the labeled MRG15 (10 nM) was added to each tube of the dilution series. Samples were mixed by pipetting up and down. The reaction mixtures were incubated for 10 min at r.t. and loaded into premium coated capillaries. Data were acquired using the MO.Control software in Binding Check, Binding Affinity, or Expert mode. MST measurements were performed at  $25\text{ }^{\circ}\text{C}$  for 20 s.

$K_D$  values were calculated from compound concentration-dependent changes in normalized fluorescence ( $F_{\text{norm}}$ ) of MRG15 after 2.5 s of MST on-time. Each binding experiment was performed in triplicate and  $K_D$  values obtained are the mean of these three independent measurements. Data were analyzed using MO Affinity Analysis software (NanoTemper Technologies).

The  $Z'$  factor<sup>28</sup> to estimate the assay quality was calculated using the following equation:

$$Z' = 1 - \frac{(3\sigma_{c+} + 3\sigma_{c-})}{|\mu_{c+} - \mu_{c-}|}$$

where  $\sigma_{c+}$  and  $\sigma_{c-}$  are standard deviations of the positive and negative control measurements, respectively, and  $\mu_{c+}$  and  $\mu_{c-}$  are the mean of the respective positive and negative signal controls.

### SPR Experiments

SPR experiments were performed on a Biacore 3000 optical biosensor (Cytiva, formerly GE Healthcare Life Sciences) equipped with a research-grade CM5 sensor chip. GST-MRG15 was immobilized (50  $\mu\text{g}/\text{mL}$  in 10 mM sodium acetate, pH 4.5) on the sensor chip surface at a flow rate of 10  $\mu\text{L}/\text{min}$  by using standard amine-coupling protocols to obtain densities of 10 kRU. One flow cell was left empty for background subtractions.

The compounds were diluted in PBS supplemented with 0.005% surfactant P20, keeping a final 1% DMSO concentration, and they were tested starting from 200  $\mu\text{M}$  as the maximum concentration. Binding experiments were performed at  $25\text{ }^{\circ}\text{C}$  by using a flow rate of 30  $\mu\text{L}/\text{min}$ , with 60 s of association monitoring and 150 s of dissociation monitoring, both with and without 0.5 mg/mL bovine serum

albumin (BSA). Regeneration of the surfaces was performed, when necessary, by a 10 s injection of 5 mM NaOH.

The simple 1:1 Langmuir binding fit model of the BIAevaluation software was used for determining equilibrium dissociation constants ( $K_D$ ) and kinetic dissociation ( $k_d$ ) and association ( $k_a$ ) constants by using eqs 3 and 4:

$$\frac{dR}{dt} = k_a \times C \times (R_{\text{max}} - R) - k_d \times R \quad (3)$$

where  $R$  represents the response unit and  $C$  is the concentration of the analyte, and

$$K_D = k_d / k_a \quad (4)$$

## Results and Discussion

The development of our MST assay started with the choice of the detection method.<sup>29</sup> In this regard, there are several possibilities: for example, the intrinsic fluorescence of the protein (given by aromatic aminoacids) can be exploited using an UV detector; otherwise, a labeling reaction between the protein and one of the available dyes can be performed, which can give a fluorescence signal in one of the three different channels (blue, green, and red). Among all these possible approaches, we preferred the use of a red dye that is one of the most reported strategies. This choice relies on the evidence that many screening compounds and reference molecules interfere at UV and blue wavelengths.<sup>30,31</sup>

In particular, we selected the NanoTemper proprietary second-generation red dye (Monolith Protein Labeling Kit RED-NHS 2nd Generation, NanoTemper Technologies) that carries a reactive NHS-ester group that reacts with primary amines of lysine residues to form a covalent bond. It is reported that the second-generation dye gives enhanced binding amplitudes and higher signal-to-noise (S/N) ratios with respect to the first-generation dye. In addition, data can be analyzed from measurements with lower MST power and shorter MST on-times.<sup>32</sup>

The labeling reaction was sequentially optimized, performing three different approaches (**Fig. 2**). First, we used a protein with a 10  $\mu\text{M}$  concentration and a 1:3 protein-dye ratio. Unfortunately, at the end of the procedure the DOL was 0.13, leading to a too low initial fluorescence (**Fig. 2A**). We then increased the protein concentration up to 20  $\mu\text{M}$ , maintaining the 1:3 protein-dye ratio (as in the first reaction). This time the obtained DOL was 0.6, within the optimal range reported, and the labeling procedure did not change the protein integrity, as shown in the Tycho NT.6 unfolding profile (**Fig. 2B**). In addition, we observed a good initial fluorescence intensity, no photobleaching, and no



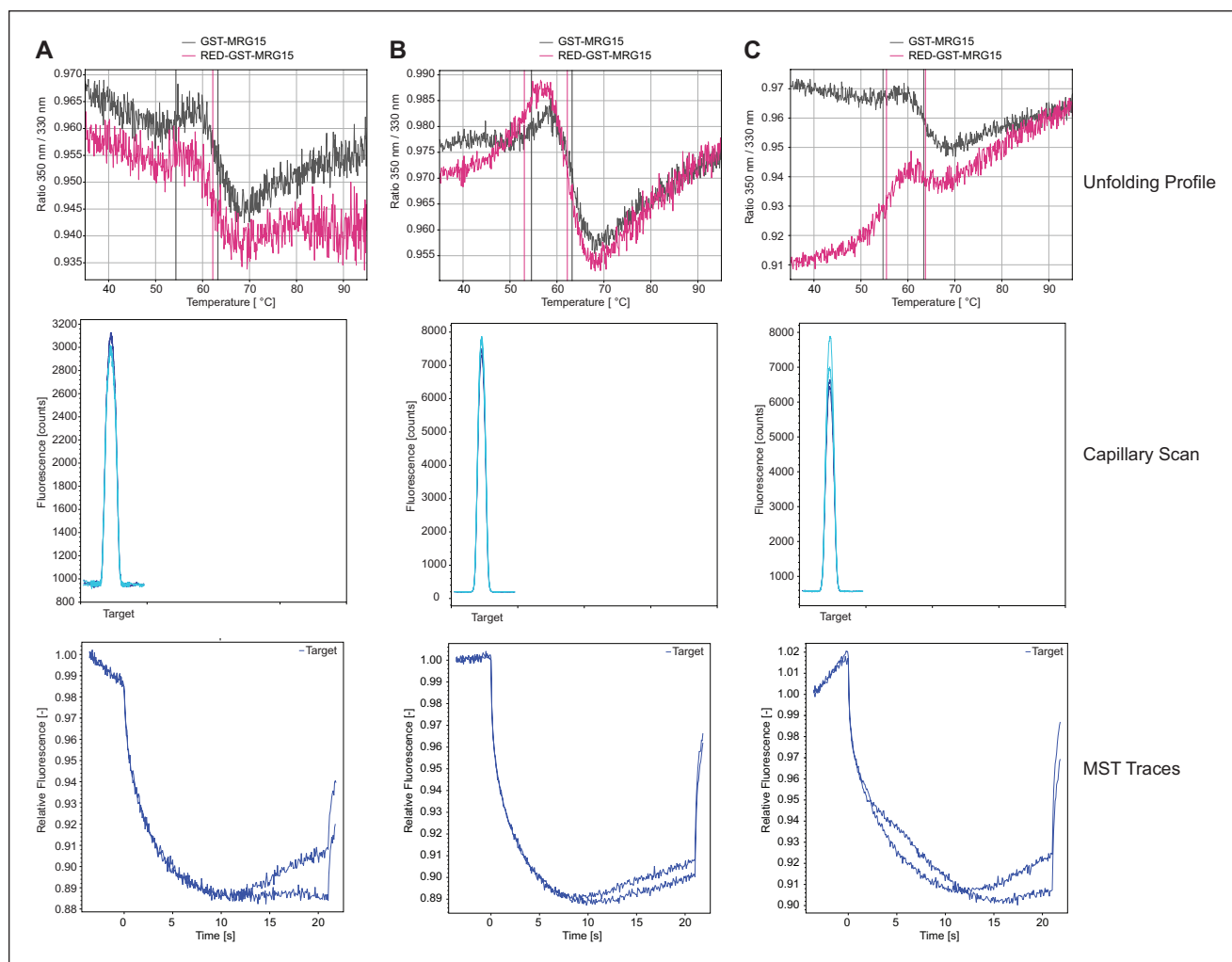


**Figure 2.** Labeling reactions performed for MRG15. Tycho NT.6 unfolding profile, capillary scan, and MST traces of MRG15 unlabeled (black) and labeled (pink) using (A) 1:3 protein–dye ratio and 10  $\mu\text{M}$  protein, (B) 1:3 protein–dye ratio and 20  $\mu\text{M}$  protein, and (C) 1:5 protein–dye ratio and 20  $\mu\text{M}$  protein.

photoenhancement. Slight variations in the two measured MST traces can be further optimized with the selection of the right assay buffer. In a next step, we tried to further optimize the labeling reaction to obtain a higher DOL and potentially improved MST traces. For this, we performed a third labeling reaction, using again the protein at 20  $\mu\text{M}$  concentration but increasing the protein–dye ratio to 1:5. In this case, we obtained a more satisfying DOL of 0.94; however, the unfolding profile of the labeled protein was different from the one of the unlabeled protein (Fig. 2C), meaning that the protein integrity changed. Moreover, protein aggregation and photoenhancement were observed, leading to the selection of the previous labeling strategy (20  $\mu\text{M}$  protein and 1:3 ratio) for further assay development.

The following step was the optimization of the assay buffer. In general, the buffer composition plays a fundamental role for both the detection of binding interactions

and the assessment of enzymatic activity.<sup>33</sup> Each protein has individual properties and requirements, such as specific pH and ionic strength values and the need for cofactors or coenzymes. All these reagents should be added to the assay buffer, and all protein requirements should be taken into account to create the most suitable environment for the protein. In addition, it is important to optimize the concentration of each reagent to be used in the buffer, as it will influence the protein behavior. Additionally, another important parameter to consider is the type of assay that has been selected to test the protein. Indeed, MST measurements are performed in small capillaries and the use of detergents such as Tween 20 or Pluronic F127 is highly recommended to avoid protein adsorption to the capillary walls.<sup>34</sup>

Therefore, being interested in the identification of optimal interaction conditions for the binding of MRG15 to small molecules, we started with the buffer optimization

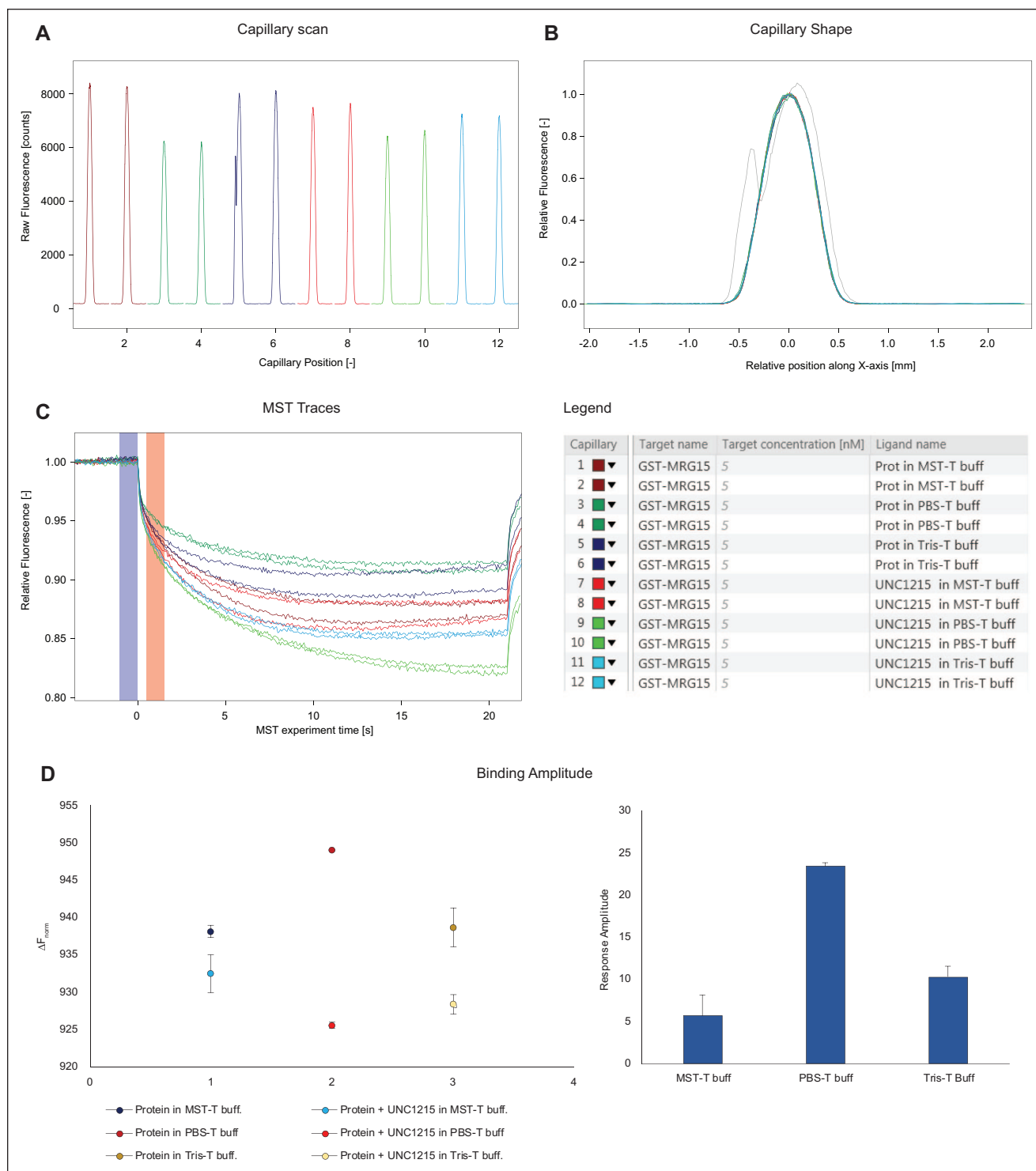


**Figure 3.** Buffer optimization. Three different buffers, MST buffer (50 mM Tris-HCl, pH 7.4, 150 mM NaCl, 10 mM MgCl<sub>2</sub>), PBS buffer, and Tris buffer (50 mM Tris-HCl, pH 8.0, 50 mM NaCl), all supplemented with 0.05% Tween 20, were tested in a single-point screening, comparing the protein alone with the protein in the presence of the reference compound (UNC1215). Four parameters were evaluated: **(A)** fluorescence intensity, **(B)** capillary shape, **(C)** trend and reproducibility of MST traces, and **(D)** binding amplitude.

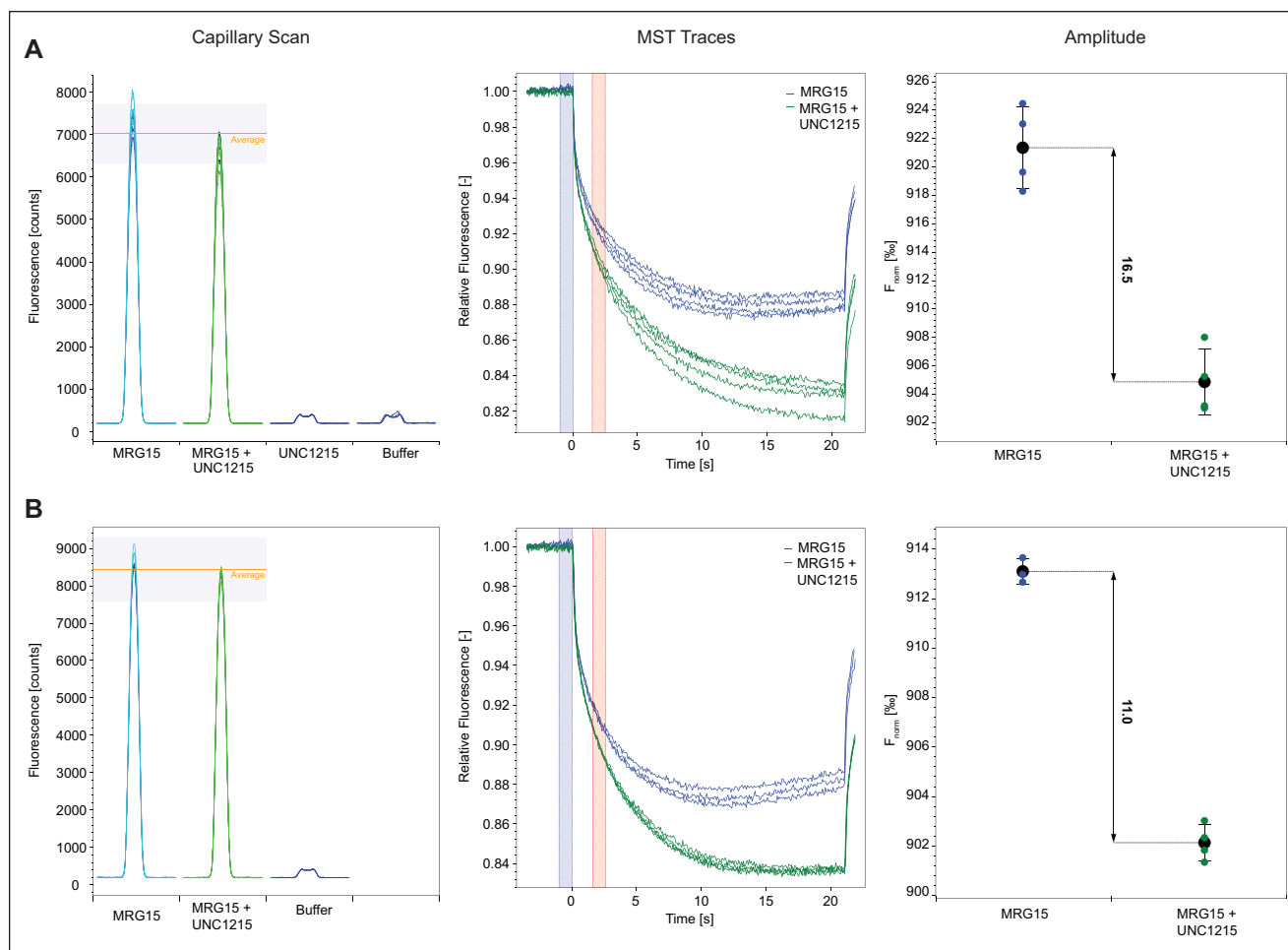


**Figure 4.** Effect of BSA on MST signal. Binding check experiment performed in **(A)** PBS buffer and **(B)** PBS buffer + 0.5 mg/mL BSA.

using the reference compound UNC1215 (**Fig. 3**). We tested three different buffers supplemented with 0.05% Tween 20 (MST buffer, PBS buffer, and Tris buffer + NaCl). Thereby we evaluated four different parameters: fluorescence intensity (**Fig. 3A**), capillary shape (**Fig. 3B**), trend and reproducibility of MST traces (**Fig. 3C**), and binding amplitude (difference between bound and unbound states) (**Fig. 3D**).

Regarding the fluorescence intensity, the capillary scan (**Fig. 3A**) showed that the use of MST buffer resulted in higher fluorescence values compared with the other two buffers, while PBS buffer gave the lowest fluorescence intensity. Regarding the capillary shape (**Fig. 3B**), we observed no signs of protein adsorption to the capillary walls, except of capillary number 5 (protein alone in Tris buffer), where we observed an atypical capillary shape, potentially related to sample adsorption. Regarding the MST traces (**Fig. 3C**), no sample aggregation was observed for any of the buffers used. However, the MST traces for the Tris buffer showed poor reproducibility.

As depicted in **Figure 3D**, the use of PBS buffer resulted in the highest amplitude value and in the lowest noise level.

Hence, considering the high amplitude, the good reproducibility of MST traces, and the well-behaved capillary shapes, PBS buffer was selected as the optimal buffer to be used for the following binding experiments.

To further optimize the buffer composition, we evaluated the eventual effect of BSA on the MST signal, as it has been reported that 0.5 mg/mL BSA can stabilize proteins in solution.<sup>35</sup>

In fact, BSA is often used in MST assays to reduce non-specific binding (NBS) on plasticware and capillary tubes, preventing the loss of material and promoting the interaction of the protein with the compounds.<sup>36</sup> Indeed, the addition of 0.5 mg/mL BSA caused a reduction of the amplitude (amplitude value of 16.5 without BSA, amplitude value of 11 with BSA), but of note, it resulted in a meaningful increase of the S/N ratio, thus behaving as a stabilizing agent for the ligand–protein interaction (**Fig. 4**). Hence, PBS buffer supplemented with BSA was used for the next experiments.

Generally, an important step in the setup of a screening approach is the establishment of the interaction of a reference

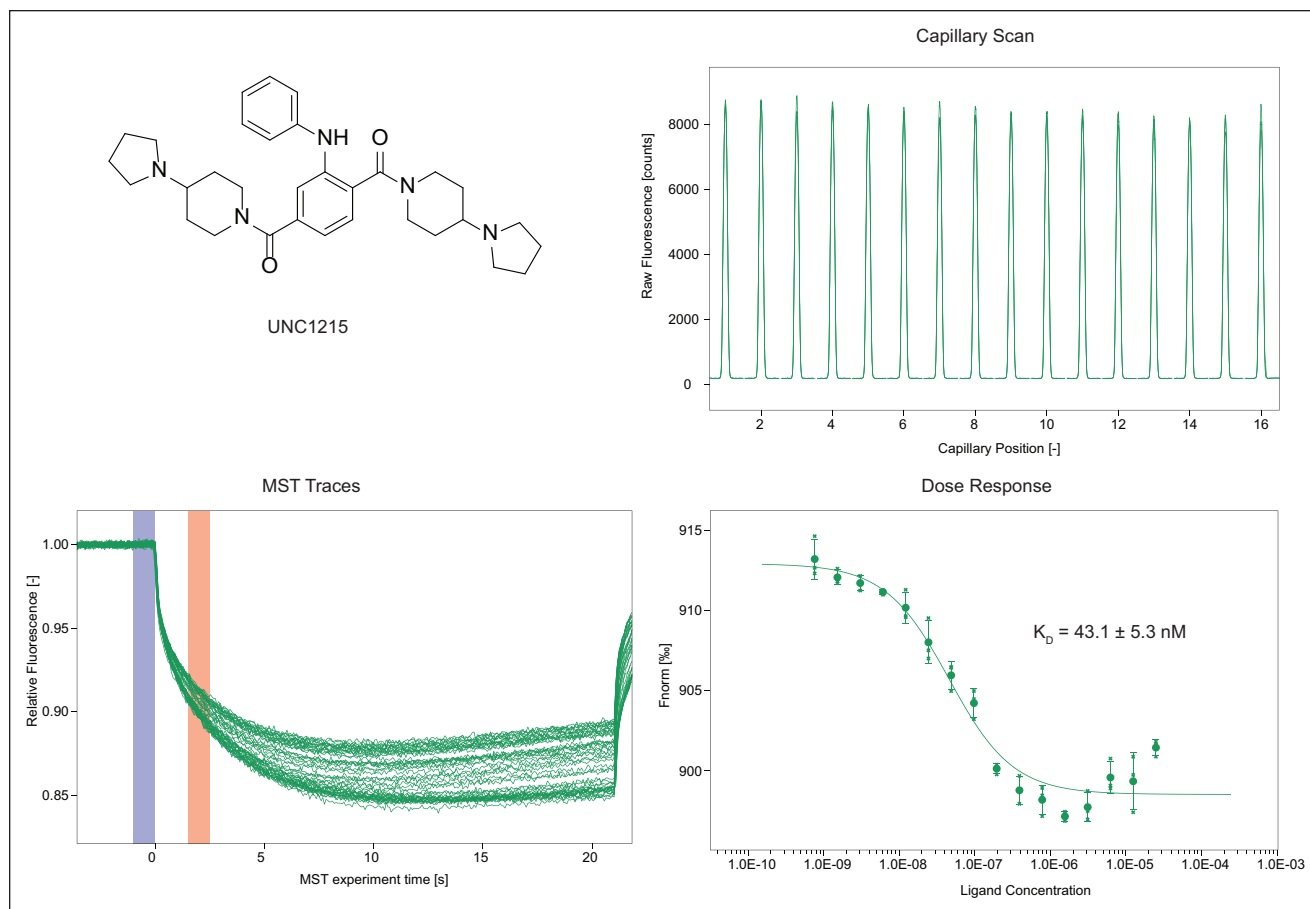


**Figure 5.** Binding experiment with the reference compound UNC1215.

molecule with the target protein in order to validate the assay selected for the screening of compounds. In our case, we used the compound UNC1215 as a reference, since it is the only reported compound capable of interacting with the protein MRG15. Regarding this compound, the  $K_D$  reported in the literature (determined by ITC)<sup>10</sup> for UNC1215 is 29.1  $\mu\text{M}$ , while in our assay we interestingly obtained a  $K_D$  of 43.1 nM (**Fig. 5**). This difference in the values obtained using two different biophysical techniques is not uncommon, since  $K_D$  values are strongly dependent on the analysis method and the experimental setup used.

After the optimization of the experimental conditions and the validation of our MST screening method by the use of a reference compound, we decided to test a small selection of compounds (**Suppl. Fig. S1**), pooled including molecules previously identified by us as ligands of reader proteins using a “library-on-library” approach (EML631, EML632, EML633, EML638, EML948, EML949, EML950, and EML951),<sup>11</sup> as well as derivatives containing methyl-lysine mimetic groups previously reported by us (EML741 and EML822)<sup>37</sup> or others (UNC0379, UNC0638, and UNC0321),<sup>38–40</sup> with the aim to verify the feasibility of the MST assay as a robust screening tool for the identification of MRG15 ligands.

The screening of the compounds was performed starting with a single-point screening (**Suppl. Fig. S2**). The compounds were tested in duplicate at a concentration of 100  $\mu\text{M}$ , using the conditions established during assay development, with positive (UNC1215) and negative (DMSO) controls included in each run. MST data obtained were then analyzed in comparison with the controls. For this, we applied a statistical differentiator of three standard deviations on either side of the mean negative control to select hit compounds, which were then further analyzed in a full 16-point titration.<sup>29</sup>

**Supplemental Figure S2** shows the results of the single-point screening, which yielded the identification of 10 hit compounds, all showing negative thermophoresis. Those compounds were further tested to determine the  $K_D$ . For this, a 16-point serial dilution series was prepared with a maximum ligand concentration of 200  $\mu\text{M}$ .

In **Supplemental Figure S3** the obtained binding curves are shown. Interestingly, we found that all the compounds identified in the primary single-point screening were able to bind the protein MRG15 with an affinity ranging from 37.8 nM to 59.1  $\mu\text{M}$  (**Table 1**). As expected, the  $K_D$  values of the three compounds that were not identified as hits after the



**Table 1.**  $K_D$  Values Obtained for Each Compound Using MST.<sup>a</sup>

Compound	Concentration, $K_D \pm SD$
<b>EML951</b>	37.8 $\pm$ 3.5 nM
<b>UNC1215</b>	43.1 $\pm$ 5.3 nM
<b>EML633</b>	248.3 $\pm$ 55.2 nM
<b>UNC0638</b>	1.7 $\pm$ 0.5 $\mu$ M
<b>EML632</b>	1.8 $\pm$ 0.3 $\mu$ M
<b>EML741</b>	2.1 $\pm$ 0.5 $\mu$ M
<b>EML948</b>	9.2 $\pm$ 0.2 $\mu$ M
<b>EML638</b>	10.3 $\pm$ 1.4 $\mu$ M
<b>EML822</b>	16.3 $\pm$ 3.3 $\mu$ M
<b>EML631</b>	18.2 $\pm$ 2.9 $\mu$ M
<b>UNC0379</b>	59.1 $\pm$ 3.4 $\mu$ M
<b>EML949</b>	>200 $\mu$ M <sup>b</sup>
<b>EML950</b>	>200 $\mu$ M <sup>b</sup>
<b>UNC0321</b>	>200 $\mu$ M <sup>b</sup>

<sup>a</sup>Each value was obtained by the mean from three independent experiments.

<sup>b</sup> $K_D$  was not determinable in the range of concentrations tested.

single-point screening were not detectable at the tested concentrations (**Table 1**, last three entries). The  $Z'$  factor of the optimized assay was calculated as greater than 0.65. These data confirm the reliability of the single-point screening approach by MST.

To validate the robustness of our MST method in the identification of MRG15 binders, we decided to repeat the binding experiments using SPR as an orthogonal assay. To this aim, MRG15 protein was immobilized on the surface of a CM5 sensor chip and the interaction of the protein was evaluated with both the reference UNC1215 and the best compound in our library, EML951. Compound UNC0321 (which was identified as a nonbinder in the previous MST single-point screening) was used as a negative control. Since BSA (0.5 mg/mL) has a crucial role in our MST assay in increasing the S/N ratio, we decided to perform SPR experiments both in the absence and in the presence of BSA, in order to investigate the eventual effects of the latter on the binding of the compounds. We found that, in the absence of BSA, both UNC1215 and EML951 bind MRG15 with  $K_D$  values of  $143.5 \pm 6.3 \mu\text{M}$  and  $137 \pm 15 \mu\text{M}$ , respectively (**Suppl. Fig. S4**), while no binding was observed for UNC0321 (**Suppl. Fig. S5**). In the presence of BSA (at the same concentration used in the MST assay), again both UNC1215 and EML951 were found to bind MRG15, yet with different  $K_D$  values (**Suppl. Fig. S4**). In particular, under these conditions the determined affinity was higher for both compounds ( $7.7 \pm 0.8 \mu\text{M}$  for UNC1215 and  $4.9 \pm 2.5 \mu\text{M}$  for EML951), therefore resulting in values closer to those obtained with MST. As depicted in **Supplemental Figure S4**, BSA affects both the association and dissociation phases, whereas no direct interaction of MRG15 with BSA was observed (**Suppl. Fig. S6**). These

results are consistent with those previously reported by others, showing that serum albumin induces an overall increase in small-molecule binding affinity for immobilized proteins in SPR experiments if compared with binding in the absence of SA.<sup>41</sup> Moreover, this is also in agreement with the fact that BSA is often used in MST assays to reduce NBS on plasticware and capillary tubes, preventing the loss of material and promoting the interaction of the protein of interest with the compounds.<sup>36</sup>

In conclusion, we developed an MST-based method that allowed the identification and subsequent  $K_D$  determination of 10 small-molecule binders for MRG15. The method is robust and convenient, especially considering its speed and low material requirements, and could be extended to other methyl-lysine or methylarginine reader proteins. Therefore, it could be a useful tool for the identification of new chemical probes to further investigate the physiopathological role of these proteins.

### Declaration of Conflicting Interests

The authors declared the following potential conflicts of interest with respect to the research, authorship, and/or publication of this article: Tanja Bartoschik is an employee of NanoTemper Technologies GmbH. Vincenzo Pisapia spent part of his PhD working in NanoTemper Technologies GmbH laboratories in Munich, and he is currently an employee of NanoTemper Technologies GmbH. The other authors declared no potential conflicts of interest with respect to the research, authorship, and/or publication of this article.

### Funding

The authors disclosed receipt of the following financial support for the research, authorship, and/or publication of this article: The Sbardella laboratory's work on epigenetics has received funding from the Italian Ministero dell'Istruzione, dell'Università e della Ricerca (MIUR), Progetti di Ricerca di Interesse Nazionale (PRIN 20152TE5PK); from the University of Salerno (FARB grant); and from Regione Campania (Italy) grant "Combattere la resistenza tumorale: piattaforma integrata multidisciplinare per un approccio tecnologico innovativo alle oncoterapie—CAMPANIA ONCOTERAPIE" (project no. B61G18000470007). Vincenzo Pisapia was funded by a PhD fellowship from the Italian Ministero dell'Istruzione, dell'Università e della Ricerca (MIUR), Programma Operativo Nazionale Ricerca e Innovazione 2014–2020, Fondo Sociale Europeo, Azione I.1 "Dottorati Innovativi con caratterizzazione Industriale."

### ORCID iD

Gianluca Sbardella  <https://orcid.org/0000-0003-0748-1145>

### References

1. Biswas, S.; Rao, C. M. Epigenetic Tools (the Writers, the Readers and the Erasers) and Their Implications in Cancer Therapy. *Eur. J. Pharmacol.* **2018**, *837*, 8–24.

2. Sbardella, G. Methyl-Readers and Inhibitors. In *Chemical Epigenetics*; Mai, A., Ed.; Springer International Publishing: Cham, 2020; pp 339–399.
3. Dawson, M. A.; Kouzarides, T.; Huntly, B. J. P. Targeting Epigenetic Readers in Cancer. *N. Engl. J. Med.* **2012**, *367*, 647–657.
4. Chen, M.; Tominaga, K.; Pereira-Smith, O. M. Emerging Role of the MORF/MRG Gene Family in Various Biological Processes, including Aging. *Ann. N.Y. Acad. Sci.* **2010**, *1197*, 134–141.
5. Zhang, P.; Du, J.; Sun, B.; et al. Structure of Human MRG15 Chromo Domain and Its Binding to Lys36-Methylated Histone H3. *Nucleic Acids Res.* **2006**, *34*, 6621–6628.
6. Zhang, P.; Zhao, J.; Wang, B.; et al. The MRG Domain of Human MRG15 Uses a Shallow Hydrophobic Pocket to Interact with the N-Terminal Region of PAM14. *Protein Sci.* **2006**, *15*, 2423–2434.
7. Bowman, B. R.; Moure, C. M.; Kirtane, B. M.; et al. Multipurpose MRG Domain Involved in Cell Senescence and Proliferation Exhibits Structural Homology to a DNA-Interacting Domain. *Structure* **2006**, *14*, 151–158.
8. Chen, M.; Takano-Maruyama, M.; Pereira-Smith, O. M.; et al. MRG15, a Component of HAT and HDAC Complexes, Is Essential for Proliferation and Differentiation of Neural Precursor Cells. *J. Neurosci. Res.* **2009**, *87*, 1522–1531.
9. Iwamori, N.; Tominaga, K.; Sato, T.; et al. MRG15 Is Required for Pre-mRNA Splicing and Spermatogenesis. *Proc. Natl. Acad. Sci. U.S.A.* **2016**, *113*, E5408–E5415.
10. James, L. I.; Barsyte-Lovejoy, D.; Zhong, N.; et al. Discovery of a Chemical Probe for the L3MBTL3 Methyl-Lysine Reader Domain. *Nat. Chem. Biol.* **2013**, *9*, 184–191.
11. Bae, N.; Viviano, M.; Su, X.; et al. Developing Spindlin1 Small-Molecule Inhibitors by Using Protein Microarrays. *Nat. Chem. Biol.* **2017**, *13*, 750–756.
12. Bai, F.; Morcos, F.; Cheng, R. R.; et al. Elucidating the Druggable Interface of Protein–Protein Interactions Using Fragment Docking and Coevolutionary Analysis. *Proc. Natl. Acad. Sci. U.S.A.* **2016**, *113*, E8051–E8058.
13. Scott, D. E.; Bayly, A. R.; Abell, C.; et al. Small Molecules, Big Targets: Drug Discovery Faces the Protein–Protein Interaction Challenge. *Nat. Rev. Drug Discov.* **2016**, *15*, 533–550.
14. Bae, N.; Gao, M.; Li, X.; et al. A Transcriptional Coregulator, SPIN-DOC, Attenuates the Coactivator Activity of Spindlin1. *J. Biol. Chem.* **2017**, *292*, 20808–20817.
15. Zhang, R.; Monsma, F. Fluorescence-Based Thermal Shift Assays. *Curr. Opin. Drug Discov. Dev.* **2010**, *13*, 389–402.
16. Gao, K.; Oerlemans, R.; Groves, M. R. Theory and Applications of Differential Scanning Fluorimetry in Early-Stage Drug Discovery. *Biophys. Rev.* **2020**, *12*, 85–104.
17. Grøftehaug, M. K.; Hajizadeh, N. R.; Swann, M. J.; et al. Protein–Ligand Interactions Investigated by Thermal Shift Assays (TSA) and Dual Polarization Interferometry (DPI). *Acta Crystallogr. D* **2015**, *71*, 36–44.
18. Nguyen, H.; Park, J.; Kang, S.; et al. Surface Plasmon Resonance: A Versatile Technique for Biosensor Applications. *Sensors* **2015**, *15*, 10481.
19. Hinman, S. S.; McKeating, K. S.; Cheng, Q. Surface Plasmon Resonance: Material and Interface Design for Universal Accessibility. *Anal. Chem.* **2018**, *90*, 19–39.
20. Drescher, D. G.; Selvakumar, D.; Drescher, M. J. Chapter One—Analysis of Protein Interactions by Surface Plasmon Resonance. In *Advances in Protein Chemistry and Structural Biology*; Donev, R., Ed.; Academic Press: Amsterdam, 2018; pp 1–30.
21. Cooper, M. A. Optical Biosensors in Drug Discovery. *Nat. Rev. Drug Discov.* **2002**, *1*, 515–528.
22. Baranauskiene, L.; Kuo, T.-C.; Chen, W.-Y.; et al. Isothermal Titration Calorimetry for Characterization of Recombinant Proteins. *Curr. Opin. Biotechnol.* **2019**, *55*, 9–15.
23. Kabiri, M.; Unsworth, L. D. Application of Isothermal Titration Calorimetry for Characterizing Thermodynamic Parameters of Biomolecular Interactions: Peptide Self-Assembly and Protein Adsorption Case Studies. *Biomacromolecules* **2014**, *15*, 3463–3473.
24. Jerabek-Willemsen, M.; André, T.; Wanner, R.; et al. MicroScale Thermophoresis: Interaction Analysis and Beyond. *J. Mol. Struct.* **2014**, *1077*, 101–113.
25. Bartoschik, T.; Maschberger, M.; Feoli, A.; et al. Microscale Thermophoresis in Drug Discovery. In *Applied Biophysics for Drug Discovery*; Huddler, D., Zartler, E. R., Eds.; John Wiley & Sons: Hoboken, NJ, 2017; pp 73–92.
26. Seidel, S. A. I.; Dijkman, P. M.; Lea, W. A.; et al. Microscale Thermophoresis Quantifies Biomolecular Interactions under Previously Challenging Conditions. *Methods* **2013**, *59*, 301–315.
27. Gupta, A. J.; Duhr, S.; Baaske, P. Microscale Thermophoresis (MST). In *Encyclopedia of Biophysics*; Springer: Berlin, **2018**; pp 1–5.
28. Zhang, J.-H.; Chung, T. D. Y.; Oldenburg, K. R. A Simple Statistical Parameter for Use in Evaluation and Validation of High Throughput Screening Assays. *J. Biomol. Screen.* **1999**, *4*, 67–73.
29. Rainard, J. M.; Pandarakalam, G. C.; McElroy, S. P. Using Microscale Thermophoresis to Characterize Hits from High-Throughput Screening: A European Lead Factory Perspective. *SLAS Discov.* **2018**, *23*, 225–241.
30. Simeonov, A.; Jadhav, A.; Thomas, C. J.; et al. Fluorescence Spectroscopic Profiling of Compound Libraries. *J. Med. Chem.* **2008**, *51*, 2363–2371.
31. Borrel, A.; Huang, R.; Sakamuru, S.; et al. High-Throughput Screening to Predict Chemical-Assay Interference. *Sci. Rep.* **2020**, *10*, 3986.
32. Bartoschik, T.; Bekic, I.; Hassemer, T.; et al. *Improved Quantitation of Biomolecular Interactions by MicroScale Thermophoresis Using the RED-NHS 2nd Generation Labeling Kit*; NanoTemper Technologies GmbH: Munich, **2018**.
33. Bisswanger, H. Enzyme Assays. *Perspect. Sci.* **2014**, *1*, 41–55.
34. Linke, P.; Amaning, K.; Maschberger, M.; et al. An Automated Microscale Thermophoresis Screening Approach for Fragment-Based Lead Discovery. *J. Biomol. Screen.* **2015**, *21*, 414–421.

35. Jerabek-Willemsen, M.; Wienken, C. J.; Braun, D.; et al. Molecular Interaction Studies Using Microscale Thermophoresis. *Assay Drug Dev. Technol.* **2011**, *9*, 342–353.
36. Scheuermann, T. H.; Padrick, S. B.; Gardner, K. H.; et al. On the Acquisition and Analysis of Microscale Thermophoresis Data. *Anal. Biochem.* **2016**, *496*, 79–93.
37. Milite, C.; Feoli, A.; Horton, J. R.; et al. Discovery of a Novel Chemotype of Histone Lysine Methyltransferase EHMT1/2 (GLP/G9a) Inhibitors: Rational Design, Synthesis, Biological Evaluation, and Co-Crystal Structure. *J. Med. Chem.* **2019**, *62*, 2666–2689.
38. Ma, A.; Yu, W.; Li, F.; et al. Discovery of a Selective, Substrate-Competitive Inhibitor of the Lysine Methyltransferase SETD8. *J. Med. Chem.* **2014**, *57*, 6822–6833.
39. Liu, F.; Chen, X.; Allali-Hassani, A.; et al. Protein Lysine Methyltransferase G9a Inhibitors: Design, Synthesis, and Structure Activity Relationships of 2,4-Diamino-7-aminoalkoxy-Quinazolines. *J. Med. Chem.* **2010**, *53*, 5844–5857.
40. Vedadi, M.; Barsyte-Lovejoy, D.; Liu, F.; et al. A Chemical Probe Selectively Inhibits G9a and GLP Methyltransferase Activity in Cells. *Nat. Chem. Biol.* **2011**, *7*, 566–574.
41. Kennedy, A. E.; Vohra, R.; Scott, J. A.; et al. Effects of Serum Albumin on SPR-Measured Affinity of Small Molecule Inhibitors Binding to Nerve Growth Factor. *Sens. Biosensing Res.* **2017**, *15*, 1–4.
42. Pettersen, E. F.; Goddard, T. D.; Huang, C. C.; et al. UCSF Chimera—A Visualization System for Exploratory Research and Analysis. *J. Comput. Chem.* **2004**, *25*, 1605–1612.